



Entanglement and thermodynamic scaling laws in quantum superabsorption

John Henry Reina

Departamento de Física, Universidad del Valle · Department of Physics, CCSE, University of Oslo

In collaboration with J.D. Álvarez-Cuartas

5th WSP Departamento de Física, Universidad Nacional/Universidad de Los Andes, Bogotá D.C., abril 17 de 2026

Outline

I: The Question

II: Model and Theoretical Framework

III: Results & Discussion

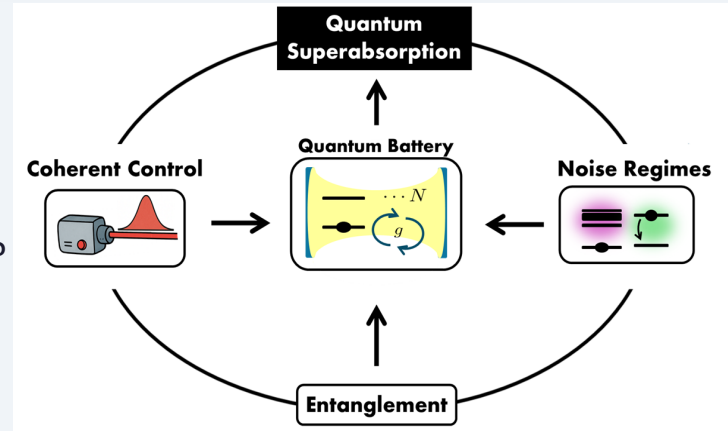
IV: Summary & Perspectives

The Open Question: What Drives Collective Enhancement?

Quach et al. (Science Advances 2022): first room-temperature superabsorption in organic microcavities (but did NOT quantify the entanglement behind the cooperative behavior).

Three questions those experiments left unanswered:

- ❓ How do entanglement correlations scale with system size N under realistic noise?
- ❓ Can dissipation act as a resource rather than a hindrance?
- ❓ Which dissipation ratio (γ^2/γ^-) yields the best thermodynamic advantage — and why?



This work:

First quantitative framework extracting finite-size scaling exponents for entanglement AND thermodynamic observables under Markovian dissipation — directly mappable to NV centers, trapped ions, organic microcavities, quantum dots, and transmon qubits.

arXiv:2510.26373v2 [quant-ph] 10 Mar 2026

Motivation: Real Platforms Already Operating in These Regimes

Quantum batteries are not a distant prospect — state-of-the-art hardware already spans the dissipation regimes we study.

Dephasing-dominated

$$\gamma^2/\gamma^- \sim 10^2$$

NV centers in diamond

T_1 : ms – s | T_2 : μ s – ms

Jarmola et al. 2012; Stanwix et al. 2010

SiC divacancies & rare-earth ions

$T_1 \gg T_2$ (dephasing-limited)

Seo et al. 2016; Alexander et al. 2022

Trapped-ion qubits

$T_1 \sim 10^3$ s | $T_2 \sim 10$ s

Zhang et al. 2025

Organic microcavities

$T_1 \sim 1$ ns | $T_2 \sim 100$ fs — room temp!

Quach et al. Science Adv. 2022 — QB superabsorption demonstrated

Intermediate

$$\gamma^2/\gamma^- \sim 10^1$$

InGaAs quantum dots in microcavities

ps dephasing | ns radiative lifetime

Bardot et al. 2005; Accanto et al. 2012

Electrons on superfluid helium

Long coherence + large dipole moment

Koolstra et al. 2025 — strong coupling to microwave resonator

Tuned-decay channels

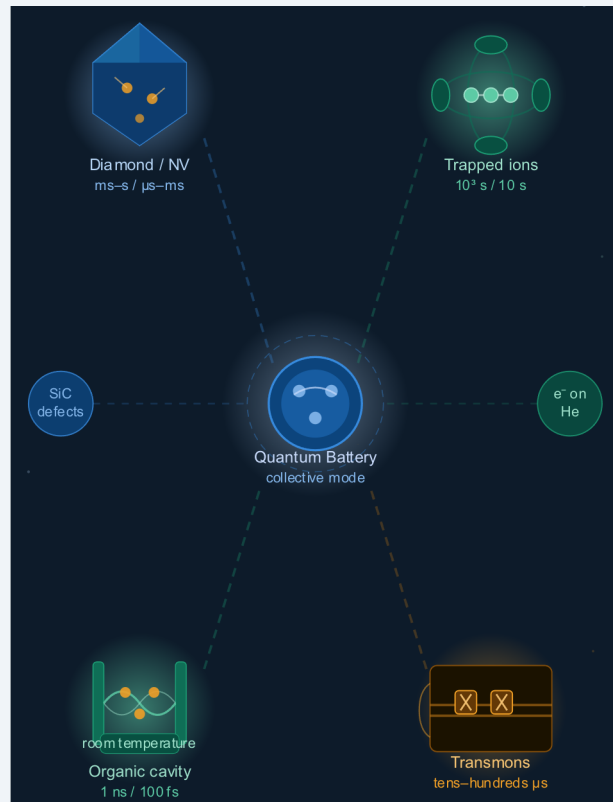
$$\gamma^2/\gamma^- \sim 10^0$$

Superconducting transmons (circuit QED)

$T_1 \sim T_2 \sim$ tens–hundreds of μ s

Hu et al. 2022; Dou & Yang 2023 — multi-qubit QB protocols demonstrated

All platforms meet our optimal window: low S_{cav} + moderate S_{qub} — natively or with standard engineering.



Theoretical Framework: Models & Observables

Two Light-Matter Models

Dicke (non-RWA)

$$\hat{H}_{\text{int}}^{(D)} = \hbar g \sum_{j=1}^N (\hat{a}^\dagger \hat{\sigma}_j^- + \hat{a} \hat{\sigma}_j^+ + \hat{a}^\dagger \hat{\sigma}_j^+ + \hat{a} \hat{\sigma}_j^-).$$

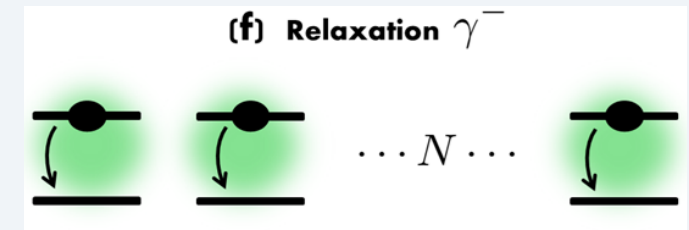
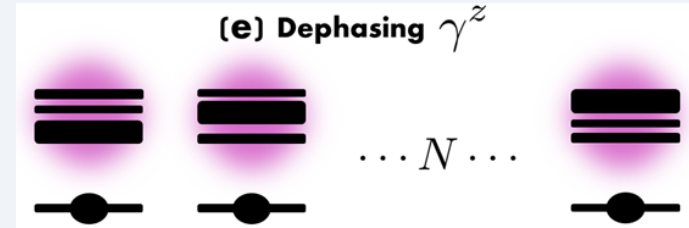
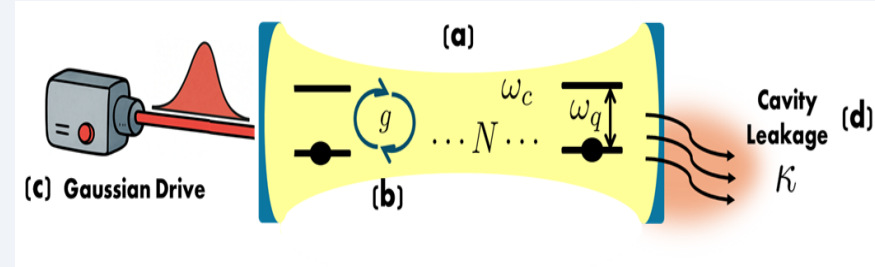
Counter-rotating terms \rightarrow ultrastrong coupling, virtual excitations, phase transitions

Tavis-Cummings (RWA)

$$\hat{H}_{\text{int}}^{(TC)} = \hbar g \sum_{j=1}^N (\hat{a}^\dagger \hat{\sigma}_j^- + \hat{a} \hat{\sigma}_j^+).$$

Excitation number conserved \rightarrow integrable, coherent Rabi oscillations

Gaussian drive on cavity: $\eta(t) = \eta_0 \exp\left(-\frac{(t-t_0)^2}{2\sigma^2}\right).$



Theoretical Framework: Models & Observables

Two Light–Matter Models

Dicke (non-RWA)

$$\hat{H}_{\text{int}}^{(\text{D})} = \hbar g \sum_{j=1}^N (\hat{a}^\dagger \hat{\sigma}_j^- + \hat{a} \hat{\sigma}_j^+ + \hat{a}^\dagger \hat{\sigma}_j^+ + \hat{a} \hat{\sigma}_j^-).$$

Counter-rotating terms \rightarrow ultrastrong coupling, virtual excitations, phase transitions

Tavis–Cummings (RWA)

$$\hat{H}_{\text{int}}^{(\text{TC})} = \hbar g \sum_{j=1}^N (\hat{a}^\dagger \hat{\sigma}_j^- + \hat{a} \hat{\sigma}_j^+).$$

Excitation number conserved \rightarrow integrable, coherent Rabi oscillations

Gaussian drive on cavity: $\eta(t) = \eta_0 \exp\left(-\frac{(t - t_0)^2}{2\sigma^2}\right).$

Key Observables

- E_{max} — maximum stored energy
- τ — charging time
- $\bar{P}_{\text{max}} = E_{\text{max}}/\tau$ — max power
- S_q, S_c — entanglement entropy

3 Dissipation Channels

Cavity leakage κ

photon loss

Relaxation γ^-

spontaneous decay

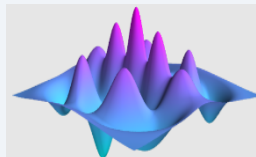
Dephasing γ^z

phase decoherence

Numerical Method: Exploiting Permutation Symmetry

Challenge: Hilbert space grows as 2^N — brute-force integration infeasible beyond $N \approx 10$

Solution: PIQS (QuTiP) exploits permutation symmetry \rightarrow Dicke subspace dimension $N+1$ instead of $2^N \rightarrow$ polynomial scaling



QuTiP

Quantum Toolbox in Python

Simulation Parameters

System sizes	$N = 5 \dots 50$ (steps of 5)
Coupling	$0 \leq g/\omega q \leq 1$
Cavity leakage	$\kappa/\omega q \in [10^{-3}, 1]$
Relaxation	$\gamma^-/\omega q \in [10^{-3}, 1]$
Dephasing	$\gamma^z/\omega q \in [10^{-3}, 1]$
Drive	Gaussian $\eta_0 = \omega q, \sigma = 2/\omega q, t_0 = 5/\omega q$

Quasi-ideal Dynamics: Energy & Entanglement vs. Coupling

Both models, $\kappa = \gamma^- = \gamma^z = 10^{-3}\omega q$ | Undriven (Fock state) and Driven (Gaussian pulse)

Dicke (non-RWA)

E_max scaling: Grows with N for $g/\omega q \gtrsim 0.5$; counter-rotating terms enhance capacity

Entanglement: Strong structured qubit–cavity correlations at $g/\omega q \gtrsim 0.5$; persist with N

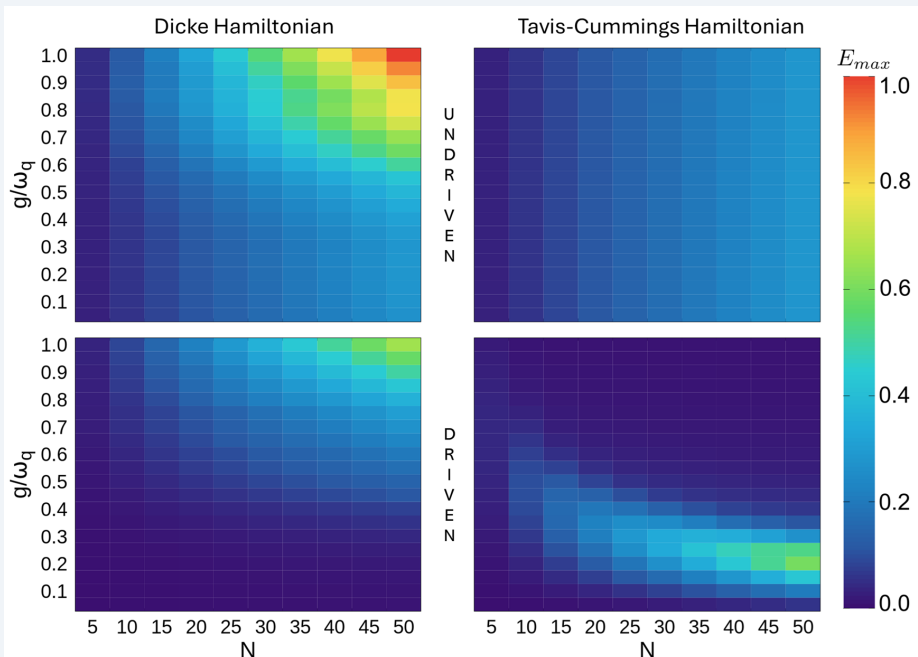
→ **Drive (role):** *Drive does not qualitatively alter Dicke dynamics — coherent energy injection without restructuring correlations*

Tavis–Cummings (RWA)

E_max scaling: Nearly vertical contours — energy depends primarily on N, not g

Entanglement: Driving amplifies correlations in narrow resonance band $g\sqrt{N} \approx \omega q/2$

→ **Drive (role):** *Drive selectively amplifies resonance — acts as entanglement initiator in the RWA regime*



Key insight: Driving acts as a controlled entanglement initiator, not a brute-force energy source.

Quasi-ideal Dynamics: Energy & Entanglement vs. Coupling

Both models, $\kappa = \gamma^- = \gamma^z = 10^{-3}\omega q$ | Undriven (Fock state) and Driven (Gaussian pulse)

Dicke (non-RWA)

E_max scaling: Grows with N for $g/\omega q \gtrsim 0.5$; counter-rotating terms enhance capacity

Entanglement: Strong structured qubit-cavity correlations at $g/\omega q \gtrsim 0.5$; persist with N

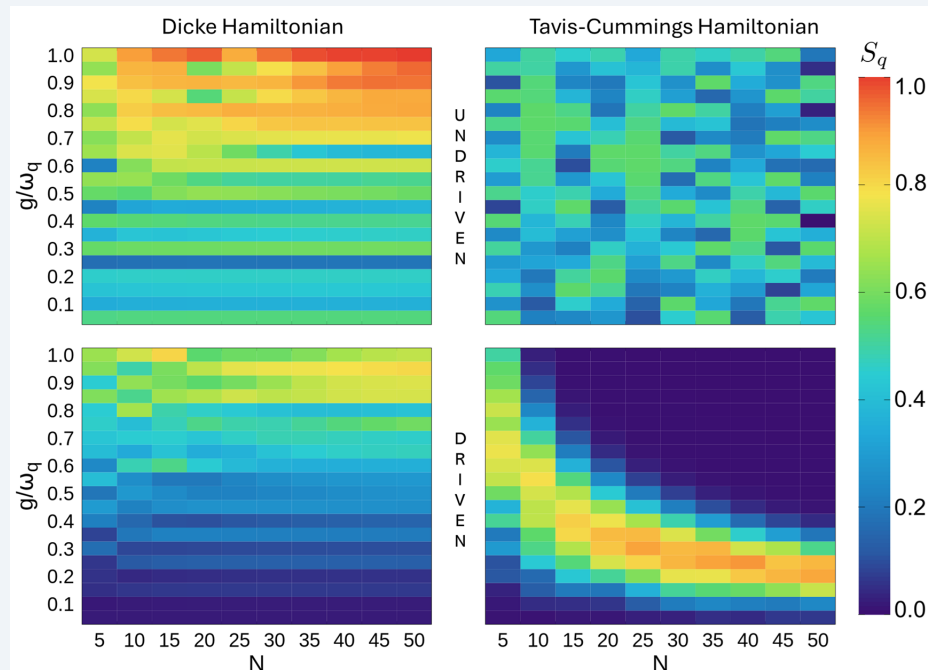
→ **Drive (role):** *Drive does not qualitatively alter Dicke dynamics — coherent energy injection without restructuring correlations*

Tavis-Cummings (RWA)

E_max scaling: Nearly vertical contours — energy depends primarily on N, not g

Entanglement: Driving amplifies correlations in narrow resonance band $g\sqrt{N} \approx \omega q/2$

→ **Drive (role):** *Drive selectively amplifies resonance — acts as entanglement initiator in the RWA regime*



Key insight: Driving acts as a controlled entanglement initiator, not a brute-force energy source.

Open-System Dynamics: Cavity Leakage & Qubit Decoherence

$$\frac{\partial \rho(t)}{\partial t} = -\frac{i}{\hbar} [H(t), \rho(t)] + \sum_{j=1}^N (\gamma^z \mathcal{L}[\sigma_j^z] + \gamma^- \mathcal{L}[\sigma_j^-] + \kappa \mathcal{L}[a])$$

Cavity Leakage (κ effects)

- TC model: nearly linear scaling in E_{\max} across ALL values of κ — robust to photon loss
- Dicke model: quickly saturates; energy grows with N only for very small κ
- Counter-rotating terms enhance capacity in quasi-ideal limit BUT accelerate degradation under cavity losses
- Entanglement entropy (Dicke): pronounced minimum at $\kappa/\omega_q \approx 0.2-0.4$ — moderate loss briefly suppresses qubit-cavity correlations

Dephasing & Relaxation interplay

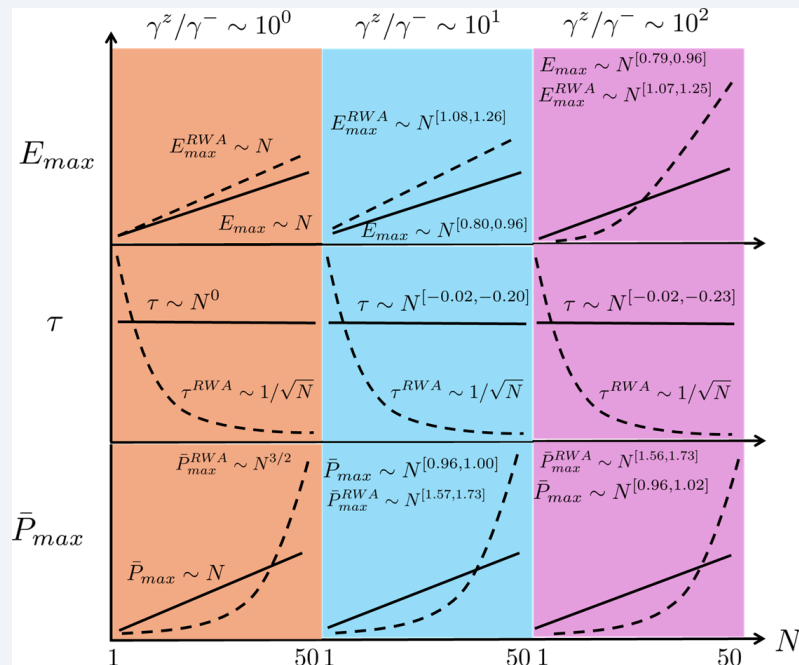
- Dicke: enhanced E_{\max} up to γ^- , $\gamma^z/\omega_q \approx 0.4$ — collective coupling amplifies noise tolerance
- TC model: broader stability domain, E_{\max} retained up to γ^- , $\gamma^z/\omega_q \approx 0.8$
- Charging time τ : nearly constant in Dicke; TC shows delays at small N but delay disappears for $N \gtrsim 30$
- Optimal window: $\gamma^-/\omega_q \lesssim 0.20$ and $\gamma^z/\omega_q \lesssim 0.50$ (both models)

Better performance \leftrightarrow intermediate S_q + low S_c . High cavity mixedness anti-correlates with E_{\max} , \bar{P}_{\max} and τ .

Finite-Size Scaling Laws: $O(N) \sim N^\alpha$

Power-law fits from log-log plots across $N = 5 \dots 50$ | $\alpha > 1 =$ quantum advantage; $\alpha \approx 1 =$ classical; $\alpha < 1 =$ degraded

Regime (γ^z/γ^-)	Model	αE_{max}	$\alpha \tau$	$\alpha \bar{P}_{max}$
$\sim 10^0$ (tuned)	Dicke	1.00	0.00	1.00
$\sim 10^0$ (tuned)	TC (RWA)	~ 1.00	-0.50	~ 1.50
$\sim 10^1$ (interm.)	Dicke	0.80–0.96	-0.02 to -0.20	0.96–1.00
$\sim 10^1$ (interm.)	TC (RWA)	1.08–1.26	≈ -0.48	1.57–1.73
$\sim 10^2$ (dephasing-dom.)	Dicke	0.79–0.96	-0.02 to -0.23	0.96–1.02
$\sim 10^2$ (dephasing-dom.)	TC (RWA)	1.07–1.25	≈ -0.49	1.56–1.73



TC model achieves genuine super-extensive scaling ($\alpha \bar{P}_{max}$ up to 1.73) in the dephasing-dominated window — driven by bipartite entanglement with the cavity.

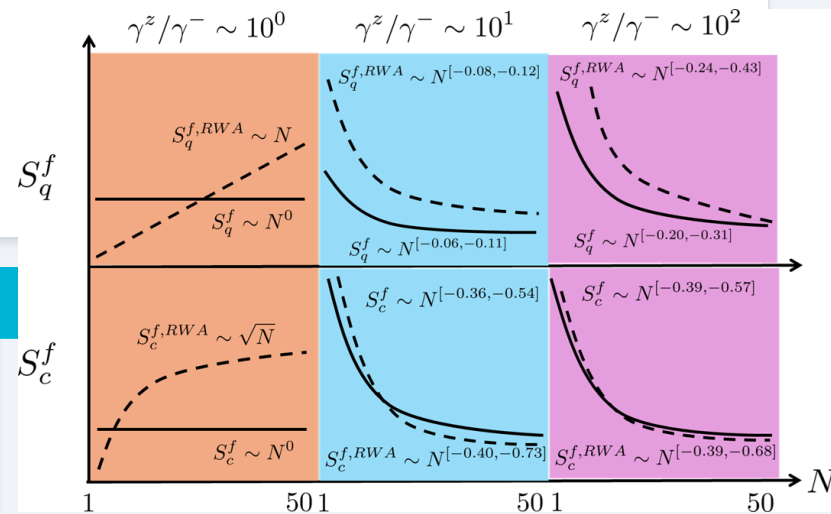
Entropy Scaling: Entanglement as the Key Resource

Dicke Model — Entropy-Suppressed Behavior

- Long-time entropies saturate: $\alpha S_f^q, \alpha S_f^c \approx 0$ (tuned-decay regime)
- Dephasing-dominated: $\alpha S_f^q \in [-0.20, -0.31], \alpha S_f^c \in [-0.39, -0.57] \rightarrow$ partial purification
- Larger $N \rightarrow$ more purified steady state: entanglement-clean operation
- Drive does not qualitatively alter this — counter-rotating terms act as internal coherence stabilizers

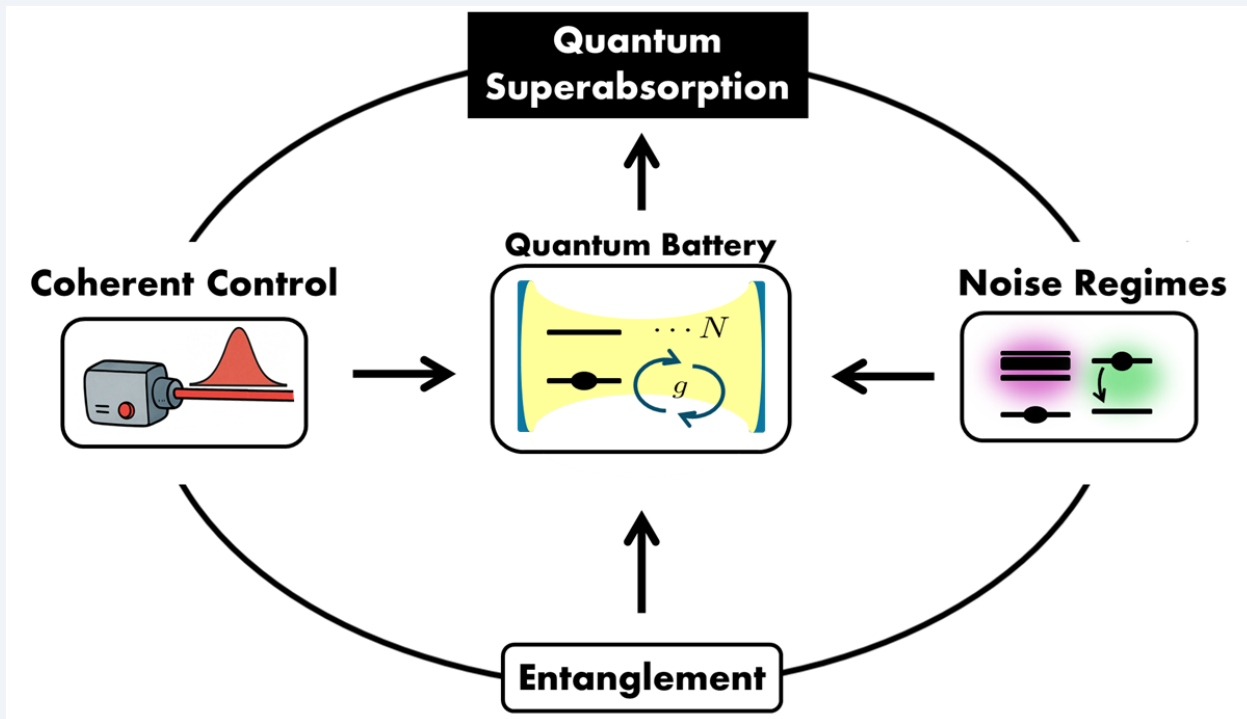
Tavis–Cummings — Entanglement-Enhanced Scaling

- Tuned-decay: cavity entropy grows weakly ($\alpha S_f^c \approx 0.2-0.4$); qubit entropy size-independent
- Dephasing-dominated: both entropies develop negative exponents \rightarrow correlations bounded and controlled
- This transition marks where dephasing stops being destructive and starts regulating entanglement buildup
- Superextensive thermodynamic performance directly tracks the growth of entanglement entropy with N



Bipartite entanglement (qubit–cavity) is the key resource underlying collective enhancement — not just a side effect

Mechanism & Outlook: Dissipation-Enhanced Superabsorption



Future Directions

- Optimal control / pulse shaping:** Tailored driving fields to maximize energy transfer while bounding entropy growth
- Non-Markovian dynamics:** Structured reservoirs (photonic crystals, correlated baths) can extend coherence and alter scaling
- Machine learning for noise:** Data-driven detection and quantification of non-Markovian processes (Scarpetta & Reina 2025)
- Many-body entanglement:** Beyond bipartite: multipartite correlations and their role in charging

Summary

01

Tavis–Cummings QB achieves genuine quantum advantage: $\alpha E_{\max} \in [1.07–1.26]$ and $\alpha \bar{P}_{\max} \in [1.56–1.73]$ in the dephasing-dominated window.

02

Dicke model: entropy-suppressed, extensive scaling — cleaner but no super-extensivity. Counter-rotating terms accelerate degradation under cavity loss.

03

Dephasing plays a dual role: limits uncontrolled entanglement growth AND reinforces superextensive thermodynamic scaling — dissipation as a resource.

04

Coherent drive acts as a coherence stabilizer (not an energy source): prevents entropy runaway while sustaining collective correlations.

05

Optimal window ($\gamma^-/\omega_q \lesssim 0.20$, $\gamma^z/\omega_q \lesssim 0.50$) maps onto NV centers, trapped ions, organic microcavities, quantum dots, and transmon qubits.

Entanglement and Dynamical Scaling Laws in Quantum Superabsorption

Juan David Álvarez-Cuartas^{1,2,*} and John H. Reina^{1,2,†}

¹*Departamento de Física and Centre for Bioinformatics and Photonics—CIBioFi, Universidad del Valle, Cali 760032, Colombia*

²*Department of Physics and Center for Computing in Science Education, University of Oslo, N-0316 Oslo, Norway*

(Dated: March 11, 2026)

Quantum batteries (QBs) exploit collective quantum resources to surpass the limits of classical energy storage and power delivery. We analyze N -qubit cavity-coupled QBs governed by Dicke and Tavis–Cummings models under Gaussian driving and open-system dynamics. Finite-size scaling laws $\mathcal{O}(N) \sim N^\alpha$ demonstrate an optimal region of relaxation and dephasing where coherent driving stabilizes entanglement entropy growth for thermodynamic observables (maximum energy E_{\max} , charging time τ , and maximum power \bar{P}_{\max}) and for qubit and cavity entanglement entropies. The Dicke model exhibits entropy-suppressed extensive behavior, while the Tavis–Cummings model achieves super-extensive scaling with $\alpha_{E_{\max}} \in [1.08, 1.26]$, $\alpha_\tau \approx -0.49$, $\alpha_{\bar{P}_{\max}} \in [1.57, 1.73]$, supported by qubit-cavity entanglement. We demonstrate that dissipation can act as a stabilizer source, yielding scaling benchmarks that are relevant to several experimental platforms. Our findings connect entanglement, dissipation-enhanced scaling laws and superabsorption, outlining a pathway towards scalable quantum batteries offering practical quantum advantage.

arXiv:2510.26373v2 [quant-ph] 10 Mar 2026 / Phys. Rev. Research (in Press)

Quantum coherence as a resource: Information thermodynamics

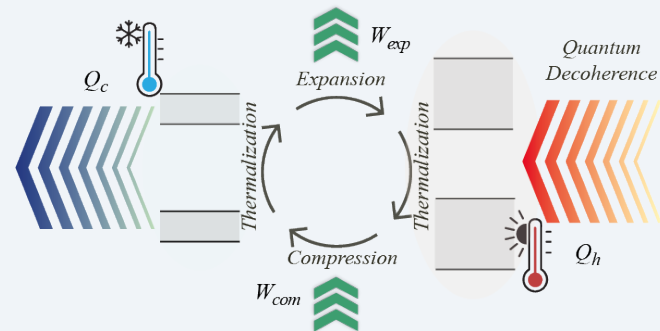
Markovian heat engine boosted by quantum coherence

Freddier Cuenca-Montenegro¹, Marcela Herrera¹, and John H. Reina^{1,2}

¹*Centre for Bioinformatics and Photonics—CIBioFi and Departamento de Física, Universidad del Valle, 760032 Cali, Colombia and*

²*Department of Physics, University of Oslo, N-0316 Oslo, Norway*

We evaluate the role of quantum coherence as a thermodynamic resource in a noisy, Markovian, one-qubit heat engine. By consuming the coherence of noisy quantum states, we demonstrate that the engine can surpass the classical efficiency limit when operating according to a quantum Otto cycle. The engine's non-classical nature is demonstrated by its violation of the Leggett-Garg's temporal correlations inequality. Amplitude damping increases the extractable work under partial thermalization, thereby increasing the efficiency. In contrast, phase damping increases the extractable work under partial thermalization but reduces the efficiency. We implement the entire Otto cycle in a quantum circuit, simulating realistic amplitude and phase damping channels, as well as gate-level noise. We introduce an operational measure of the circuit's thermodynamic cost to establish a direct link between energy consumption and information processing in quantum heat engines.



Quantum Otto cycle for a one-qubit heat engine: The cycle comprises two isochoric and two adiabatic strokes.

arXiv:2505.22902v2 [quant-ph] 6 Mar 2026 / Phys. Rev. A (under revision)

Ongoing collaborations

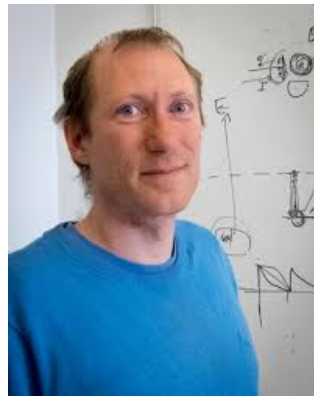
- Resource theory/information thermodynamics: CQT, Singapore (A. Ducuara, Mile Gu)
- Quantum sensing (theory and experiment): Oslo (J. Bergli, K. Tapliyal, D. Rivas)
- Quantum machine learning: Oslo (M. Hjorth-Jensen)



Juan David Álvarez



Justin Wells



Joakim Bergli



Morten Hjorth-Jensen



Juan Manuel Scarpetta



Kishore Tapliyal



Andrés F. Ducuara



David Rivas

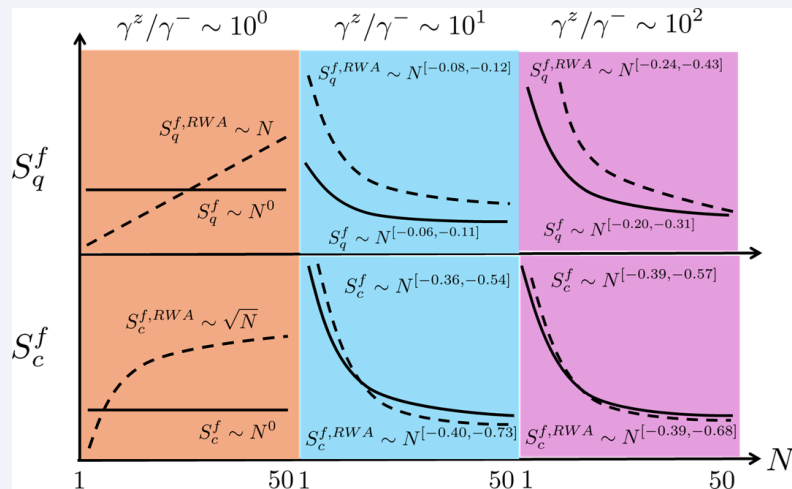


Gracias!

Finite-Size Scaling Laws: $O(N) \sim N^\alpha$

Power-law fits from log-log plots across $N = 5 \dots 50$ | $\alpha > 1 =$ quantum advantage; $\alpha \approx 1 =$ classical; $\alpha < 1 =$ degraded

Regime (γ^z/γ^-)	Model	αE_{\max}	$\alpha \tau$	$\alpha \bar{P}_{\max}$
$\sim 10^0$ (tuned)	Dicke	1.00	0.00	1.00
$\sim 10^0$ (tuned)	TC (RWA)	~ 1.00	-0.50	~ 1.50
$\sim 10^1$ (interm.)	Dicke	0.80–0.96	-0.02 to -0.20	0.96–1.00
$\sim 10^1$ (interm.)	TC (RWA)	1.08–1.26	≈ -0.48	1.57–1.73
$\sim 10^2$ (dephasing-dom.)	Dicke	0.79–0.96	-0.02 to -0.23	0.96–1.02
$\sim 10^2$ (dephasing-dom.)	TC (RWA)	1.07–1.25	≈ -0.49	1.56–1.73



TC model achieves genuine super-extensive scaling ($\alpha \bar{P}_{\max}$ up to 1.73) in the dephasing-dominated window — driven by bipartite entanglement with the cavity.

Entropy Scaling: Entanglement as the Key Resource

Dicke Model — Entropy-Suppressed Behavior

- Long-time entropies saturate: αS_{f_q} , $\alpha S_{f_c} \approx 0$ (tuned-decay regime)
- Dephasing-dominated: $\alpha S_{f_q} \in [-0.20, -0.31]$, $\alpha S_{f_c} \in [-0.39, -0.57]$ \rightarrow partial purification
- Larger $N \rightarrow$ more purified steady state: entanglement-clean operation
- Drive does not qualitatively alter this — counter-rotating terms act as internal coherence stabilizers

Tavis–Cummings — Entanglement-Enhanced Scaling

- Tuned-decay: cavity entropy grows weakly ($\alpha S_{f_c} \approx 0.2\text{--}0.4$); qubit entropy size-independent
- Dephasing-dominated: both entropies develop negative exponents \rightarrow correlations bounded and controlled
- This transition marks where dephasing stops being destructive and starts regulating entanglement buildup
- Superextensive thermodynamic performance directly tracks the growth of entanglement entropy with N

Bipartite entanglement (qubit–cavity) is the key resource underlying collective enhancement — not just a side effect.

Quasi-ideal Dynamics: Energy & Entanglement vs. Coupling

Both models, $\kappa = \gamma^- = \gamma^z = 10^{-3}\omega q$ | Undriven (Fock state) and Driven (Gaussian pulse)

Dicke (non-RWA)

E_max scaling: Grows with N for $g/\omega q \gtrsim 0.5$; counter-rotating terms enhance capacity

Entanglement: Strong structured qubit–cavity correlations at $g/\omega q \gtrsim 0.5$; persist with N

→ **Drive (role):** *Drive does not qualitatively alter Dicke dynamics — coherent energy injection without restructuring correlations*

Tavis–Cummings (RWA)

E_max scaling: Nearly vertical contours — energy depends primarily on N, not g

Entanglement: Driving amplifies correlations in narrow resonance band $g\sqrt{N} \approx \omega q/2$

→ **Drive (role):** *Drive selectively amplifies resonance — acts as entanglement initiator in the RWA regime*

Key insight: Driving acts as a controlled entanglement initiator, not a brute-force energy source.